
D-TRATTUNET: DUAL-DECODER TRANSFORMER-BASED ATTENTION UNET ARCHITECTURE FOR BINARY AND MULTI-CLASSES COVID-19 INFECTION SEGMENTATION *

A PREPRINT

Fares Bougourzi

National Research Council of Italy, 73100 Lecce, Italy
and University Paris-Est Creteil, Laboratoire LISSI, 94400
Vitry sur Seine, Paris, France
faresbougourzi@gmail.com

Cosimo Distante

Institute of Applied Sciences and Intelligent
Systems, National Research Council of Italy,
73100 Lecce, Italy
Department of Innovation Engineering, University
of Salento, 73100 Lecce, Italy
cosimo.distante@cnr.it

Fadi Dornaika

Ho Chi Minh City Open Univesity,
97 Vo Van Tan, Ward Vo Thi Sau, District 3,
Ho Chi Minh City, 70000, Vietnam
fdornaika@gmail.com

Abdelmalik Taleb-Ahmed

IEMN UMR CNRS 8520, Université
Polytechnique Hauts de France, UPHF
Abdelmalik.Taleb-Ahmed@uphf.fr

March 29, 2023

ABSTRACT

In the last three years, the world has been facing a global crisis caused by Covid-19 pandemic. Medical imaging has been playing a crucial role in the fighting against this disease and saving the human lives. Indeed, CT-scans has proved their efficiency in diagnosing, detecting, and following-up the Covid-19 infection. In this paper, we propose a new Transformer-CNN based approach for Covid-19 infection segmentation from the CT slices. The proposed D-TrAttUnet architecture has an Encoder-Decoder structure, where compound Transformer-CNN encoder and Dual-Decoders are proposed. The Transformer-CNN encoder is built using Transformer layers, UpResBlocks, ResBlocks and max-pooling layers. The Dual-Decoder consists of two identical CNN decoders with attention gates. The two decoders are used to segment the infection and the lung regions simultaneously and the losses of the two tasks are joined.

The proposed D-TrAttUnet architecture is evaluated for both Binary and Multi-classes Covid-19 infection segmentation. The experimental results prove the efficiency of the proposed approach to deal with the complexity of Covid-19 segmentation task from limited data. Furthermore, D-TrAttUnet architecture outperforms three baseline CNN segmentation architectures (Unet, AttUnet and Unet++) and three state-of-the-art architectures (AnamNet, SCOATNet and CopleNet), in both Binary and Mutli-classes segmentation tasks.

Keywords Covid-19 · Transformer · Convolutional Neural Network · Deep Leaning · Segmentation · Unet

1 Introduction

Since December 2019, the world has been in a global crisis due to the spread of Covid-19 disease. The first step in the fight against this pandemic is to detect and isolate the infected person to stop the infection cycle. In fact, RT-PCR test

*This work has been submitted to the IEEE for possible publication. Copyright may be transferred without notice, after which this version may no longer be accessible.

has been considered as the golden standard for detecting the infected individuals. However, this test has a considerable false-negative rate [1, 2]. On the other hand, RT-PCR test has very limited use for following up the patient's state and the progression of the disease [3–5]. To deal with these issues medical imaging modalities have been widely used as major or supporting tool [6].

CT-scans have been widely used for Covid-19 analysis. CT-scans are a very informative screening tool, thus, it can be used for Covid-19 detection [3, 4], Segmentation [5], Severity prediction [7] and Covid-19 infection percentage estimation [8]. Covid-19 infection segmentation is very important to recognize the infection and following up the patient's state [9–11]. However, developing an efficient machine learning approach to segment the infection is very challenging task [12–14].

The main challenge in segmenting Covid-19 infections is the lack of an adequate data to train machine learning models [14, 15], especially deep learning methods, which requires huge labelled data [16, 17]. On the other hand, the infection has high variability in intensity, shape, position and type, which makes the segmentation task very challenging [18, 19]. Covid-19 infection stage (early vs advanced), symptoms (asymptomatic vs symptomatic patients), and severity are additional factors that complicate the segmentation task [20]. In more details, the infection usually appears as ground-glass opacification (GGO) especially in the early stages [20, 21]. Generally, GGO has blurred edges and low contrast with the surrounding lung tissues [20, 21]. In later stages, the infection usually appears as a mixture of GGO and consolidation. At these stages, the infection segmentation challenges are compound of the blurred edges and low contrast of GGO, and the resemblance between the consolidation, the lungs walls and the other lung tissues [20, 21].

In the literary, Covid-19 infection segmentation can be categorized as Binary segmentation (infection or non-infection) [9, 12, 13, 22] or Multi-classes segmentation (non-infection, GGO or consolidation) [10, 14]. Binary segmentation is quantitative segmentation that shows how much the infection is spread in the lungs. On the other hand, the multi-classes segmentation provides information not only about the degree of infection spread, but it gives better idea about the stage, progress and severity of the infection [5, 10, 14]. Despite, the big importance of segmenting different infection classes, only few works have addressed this task due to data limitation for multi-classes Covid-19 segmentation [10, 14].

The aim of this work is exploit the recent strengths of both CNNs and Transformers to provide an efficient solution for Covid-19 infection segmentation as binary and Multi-classes segmentation tasks. The proposed approach has demonstrated its efficiency in extracting local context information, long-range dependencies, and global context information through the proposed CNN-Transformer encoder. To guide the models to concentrate inside the lungs and discard non-lung tissues, Dual Decoders is proposed for segmenting the infection and the lungs simultaneously. In summary, the main contributions of this paper are:

- A hybrid CNN-Transformer network is proposed that leverages the strengths of Transformers and CNNs to extract high-level features during the encoding phase.
- The proposed D-TrAttUnet encoder consists of two paths; the Transformer path and the Unet-like Fusion path. The Transformer path considers 2D patches of the input image as input, and consecutive Transformer layers to extract high representations at different levels. Four different Transformer features at different levels are injected into the Unet-like Fusion Encoder through UpResBlocks. On the other hand, the first layer of the Unet-like path uses the convolutional layers on the input image. The following Unet-Like Fusion layers combine the Transformer features with the previous layer of the Unet-Like path through concatenation and ResBlocks.
- The proposed D-TrAttUnet decoder consists of dual identical decoders. The objective of using two decoders is to segment Covid-19 infection and the lung regions simultaneously. Each decoder has four Attention Gates (AG), ResBlocks and bilinear Upsampling layers similar to the Attion Unet (AttUnet) architecture, taking advantage of CNN-Transformer and multi-task tricks.
- To evaluate the performance of our proposed architecture, both binary infection segmentation and multi-classes infection segmentation are investigated using three publicly available datasets.
- The comparison with three baseline architectures (Unet [23], Att-Unet [24], and Unet++ [25]) and three state-of-the-art architectures for Covid-19 segmentation (CopleNet [12], AnamNet [13], and SCOATNet [10]), demonstrates the superiority of our proposed D-TrAttUnet architecture in both Binary and Multi-classes Segmentation tasks. The codes of the proposed D-TrAttUnet will be publicly available at. <https://github.com/faresbougourzi/D-TrAttUnet>.

This paper is organised as follows: Section 2 presents some related work on CNN-based and Transformer-based segmentation architectures and segmentation of Covid-19 infections from CT scans. In section 3, we describe our proposed approach. Section 4 consists of the description of the datasets used and the evaluation metrics. Section 5

presents and discusses the experiments and results. Section 6 shows some segmentation examples. Finally, section 7 concludes this paper.

2 Related Work

In this section, we will briefly describe the related works on three aspects: CNN-based segmentation architectures, Transformers in computer vision and some Covid-19 infection segmentation state-of-the-art approaches.

2.1 CNN Segmentation Architectures

Since the great success of the first deep CNN architecture “Alexnet” [26] in ImageNet [27] challenge in 2012, CNNs have reached the state of the art performance in many computer vision and machine learning tasks [16,17]. Segmentation tasks have been influenced by the great success of the CNNs and therefore many CNN architectures have proved their ability to segment many complicated medical imaging tasks [23,28,29]. Since Unet architecture [23] was proposed in 2017, great progress has been made and a lot of Unet variants have been proposed such as Attention Unet (Att-Unet) [24], Unet++ [25], ResUnet [30].

Unet [23] is a CNN architecture with Encoder-Decoder structure. Unet’s encoder consists of consecutive CNN layers. Each layer contains convolutional and maxpooling layers. On the other hand, the decoder consists of consecutive deconvolutional layers. The encoder and decoder are connected by skip connections, where encoder feature maps are concatenated with the decoder features to maintain fine-grained details by passing them to the decoder. This forms the “U-shape”. In [24], O. Oktay et al. proposed Attention Gate (AT) to determine the salient regions by using the encoder and decoder feature maps simultaneously.

2.2 Transformers in CV

Transformers are capable of capturing long-range dependencies between sequence elements. Therefore, Transformers are widely used in the Natural Language Processing (NLP) domain [31]. Inspired by the great success in the NLP domain, transformers have also been extensively studied in the computer vision domain in the last two years. [31]. Transformers have shown promising results in many computer vision tasks and many transformer-based architectures have been proposed such as ViT [32], Swin Transformer [33], and Deit [34].

Similarly, Transformers have got much interest in Medical imaging domain [35]. Indeed, Transformers have shown promising performance in many medical imaging tasks such as classification [36], detection [37] and segmentation [38]. Since the focus of this work is segmentation task, some transformer-based segmentation approaches will be describes. The segmentation architectures can be classified as 2-D [39,40] or 3-D modalities [38,41].

In [39], H. Wu et al. proposed a CNN-Transformer architecture called “Fat-Net”, where two encoders (CNN and Transformer encoders) are used. The feature maps of the two decoders were concatenated to have richer features from the two encoders. The Squeeze and Excitation (SE) module [42] was applied on the concatenated features to identify the most important feature correlations from different feature channels. Fat-Net was evaluated for skin lesion segmentation using four public datasets. In the U-Transformer [40] architecture, Multi-Head Self-Attention and Cross Attention modules were injected into the Unet architecture. These two modules were placed at the skip connection to learn the global context information from the Unet encoder and pass them to its decoder [40]. The U-Transformer architecture performed well in two abdominal CT-image datasets [40]. In [38], A. Hatamizadeh et al. proposed a transformer-based architecture for multi-classes 3D segmentation called “UNETR”. The encoder of UNETR was constructed by a transformer, from which four levels features are obtained and rescaled by deconvolutional layers. The rescaled maps were connected to the CNN decoder via skip connections at different resolutions, forming the “U-shape”.

2.3 Covid-19 infection Segmentation

Since the emergence of the infectious respiratory virus SARS-CoV-2 at the end of 2019 (in Wuhan, China), numerous machine learning approaches have been proposed to combat this deadly disease. CT -Scans along with machine learning approaches have been widely used for diagnosis [2,43,44], severity prediction [7], and quantification of covid-19 infection [8,45].

In Covid-19 analysis, segmentation of Covid-19 infections is one of the most studied tasks in the last three years [14]. Indeed, CNN-based architectures have achieved the state of the art performance in Covid-19 infection segmentation [9,10,12,13,46]. In [12], G. Wang et al. propose a segmentation architecture for segmenting COVID -19 infection lesions called “COPE-Net”.The COPE-Net architecture is a Unet variant in which a combination of max-pooling

and average-pooling is introduced in the encoding phase. Moreover, a bridge module was applied to the encoder output to improve its semantic representation and learn multiple lesion scale features. In addition, COPLE-Net was designed to learn from noisy data that were not labelled by radiologists.

AnamNet [13] is a lightweight CNN with 7.8 times fewer parameters than Unet. Therefore, AnamNet is easy to train and has low inference time which makes it suitable even for mobile devices. On the other hand, AnamNet has a Unet-like structure with a proposed AD-block inserted after the downsampling block of the encoder and the upsampling block of the decoder. In short, the AD-block was built using one by one convolutional depthwise squeezing layer, followed by another three by three convolutional layer, and finally one by one convolutional layer was used for depthwise stretching. In [10], S. Zhao et al. proposed a Unet++ [25] variant architecture called ‘‘SCOATNet’’, in which a new spacial-wise and channel-wise attention modules are proposed. The attention modules were inserted between the dense convolutional blocks of the skip pathways of the Unet++ architecture.

3 The Proposed Approach

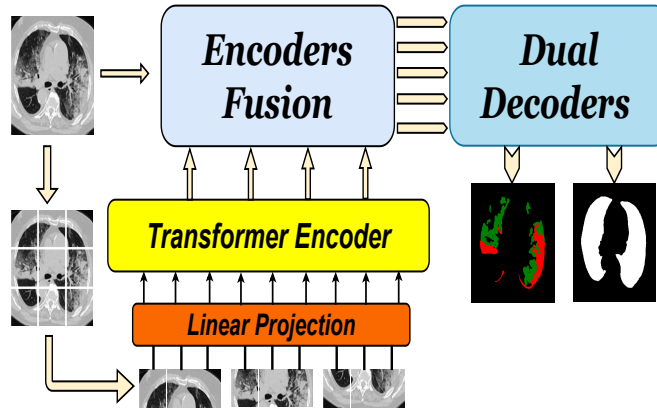


Figure 1: The summary of our proposed D-TrAttUnet approach.

The general structure of our proposed approach for Covid-19 segmentation is summarized in Figure 1. The proposed D-TrAttUnet architecture is a compound CNN Transformer architecture with Unet-like shape and exploiting the Attention Gate (AG). Figure 2 shows the detailed structure of the proposed D-TrAttUnet. The encoder of D-TrAttUnet exploits both the transformer layers and ResBlocks to extract rich features. Since Covid-19 infection problem has high variability in shape, size and position [18–20], it is important to extract richer features from the input images. Our approach combines the extracted local features using CNN layers and global features using Transformer layers.

In our proposed D-TrAttUnet, the encoder has two paths: the Unet-like path and the Transformer path. The input image $x \in \mathbb{R}^{H \times W \times C}$, where H , W and C are the height, the width and the input channels, is fed into both paths. For the transformer path, x is divided into uniform, non-overlapping patches $x_v \in \mathbb{R}^{N(S^2 \times C)}$, where $(S \times S \times C)$ is the patch size and N is the number of the patches $N = (H \times W)/S^2$. These patches are projected into embedding space z_0 using a convolutional kernel $E \in \mathbb{R}^{(S^2 \cdot C) \times K}$, where K is the dimensionality of the embedding space, which is fixed for all of the transformer layers. z_0 is defined by:

$$z_0 = [x_v^1 E; x_v^2 E; \dots; x_v^N E] \quad (1)$$

The embedded features $z_0 \in \mathbb{R}^{N \times K}$ are fed into Transformer layers similar to [32, 47]. As shown in Figure 3-c, the Transformer layer consists of two Layernorm (LN) blocks, Multi-Head Self-Attention (MSA) block, a multilayer perceptron (MLP) block and residual connections. For the Transformer layer (l), the embedded input features z_{l-1} are fed into Layernorm (LN), followed by a Multi-Head Self-Attention block, which is then summed with z_{l-1} by a residual connection, as depicted in equation (2):

$$z'_l = MSA(LN(z_{l-1})) + z_{l-1} \quad (2)$$

The embedded features of z_{l-1} which were passed by the first LN are denoted by $s = LN(z_{l-1})$. These feature maps are divided into equal features of h heads, $s = [s_1, s_2, \dots, s_h]$, each has K/h dimension features. MSA is defined by:

$$MSA = U_{msa}([SA_1(s_1); SA_2(s_2); \dots; SA_h(s_h)]) \quad (3)$$

where SA_1, SA_2, \dots, SA_h are Self-Attention Blocks, and $U_{msa} \in \mathbb{R}^{K \times K}$ is weighting matrix for the SA features.

The z'_l is fed into Layernorm (LN) block followed by MLP block then summed with z_{l-1} by residual connection, as depicted in equation (4):

$$z_l = MLP(LN(z'_l)) + z'_l \quad (4)$$

where MLP consists of two Linear layers with a GELU non-linearity. The first Linear layer ($MLP_1 \in \mathbb{R}^{K \times K_{MLP}}$) projects $LN(z'_l)$ into K_{MLP} , then the second Linear layer ($MLP_2 \in \mathbb{R}^{K_{MLP} \times K}$) projects it back to K features.

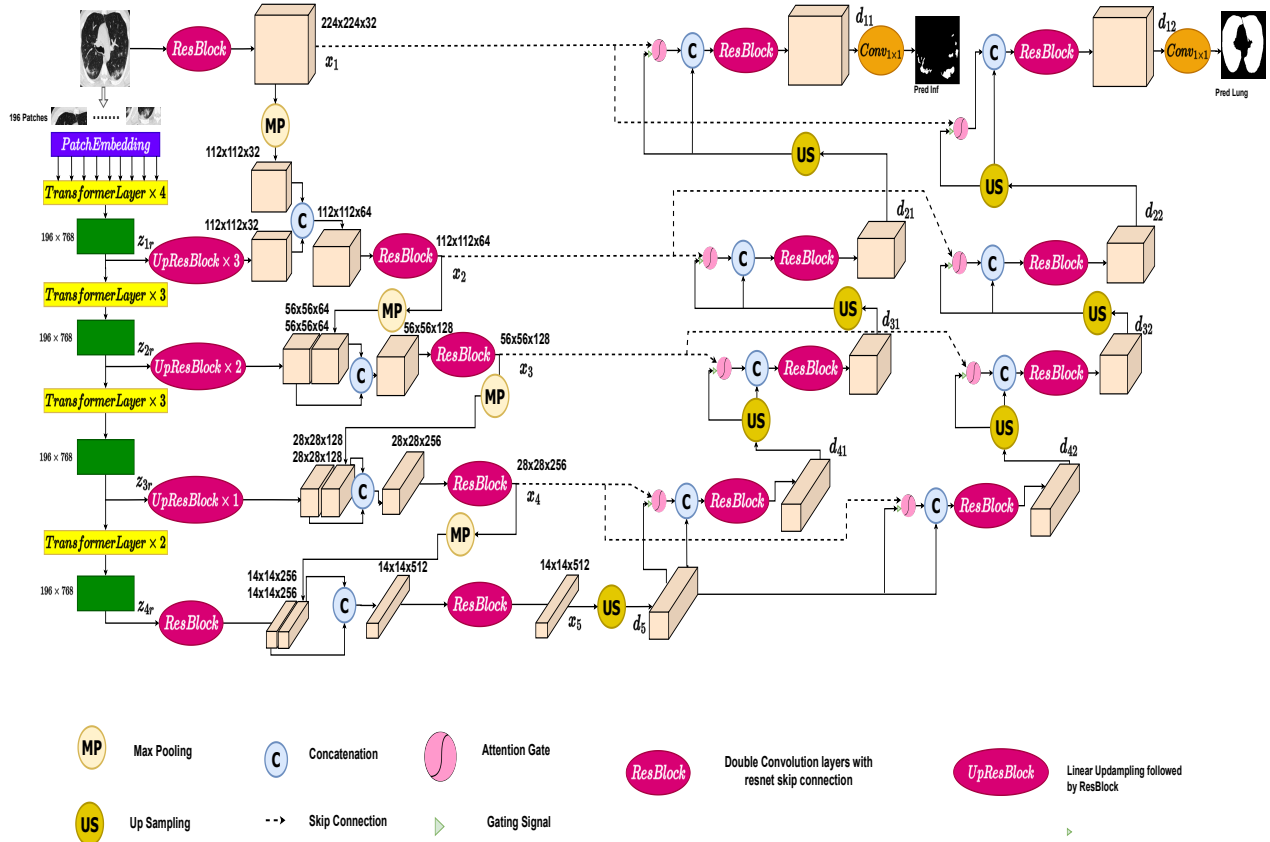


Figure 2: Detailed Structure of the proposed D-TrAttUnet architecture.

In our approach, L is set to 12, h to 12, $K = 786$, $K_{MLP} = 3072$ and $S=16 \times 16$ pixels. Consequently, $W = H = 224$, the number of patches = 196.

To obtain diversity of learned features from different Transformer layers (levels), the embedded features of layers 4, 7, 10 and 12 are selected. These layers are denoted as Tr_1, Tr_2, Tr_3 and Tr_4 , respectively. Consequently, four layers from the Transformer path were injected into D-TrAttUnet, all of which have the shape 196×786 . To have 3D shape, z_l is reshaped to $14 \times 14 \times 786$, since $14 \times 14 = 196$. The reshaped features embedded features for Tr_1, Tr_2, Tr_3 and Tr_4 are denoted by z_1, z_2, z_3 and z_4 , respectively. To inject the transformer features into different layers of D-TrAttUnet and combine them with the CNN layers, UpResBlock is introduced as depicted in Figure 3-b. UpResblock consists of linear upsampling followed by ResBlock as depicted in Figure 3-a. ResBlock consists of two 3 by 3 convolutional block, each followed by Batch Normalization and ReLU activation function. In addition, the input is

added with the output of two convolutional layers using the residual connection, which consists of 1 by 1 convolutional block, followed by Batch Normalization and ReLU activation function, as shown in equations (5) and (6):

$$x_{out_1} = ReLU(BN(Conv3 \times 3_1(x_{in}))) \quad (5)$$

$$x_{out} = ReLU(BN(Conv3 \times 3_2(x_{out_1}))) + ReLU(BN(Conv1 \times 1(x_{in}))) \quad (6)$$

where $Conv3 \times 3_1 \in \mathbb{R}^{3 \times 3 \times C_{out}}$, $Conv3 \times 3_2 \in \mathbb{R}^{3 \times 3 \times C_{out}}$ and $Conv1 \times 1 \in \mathbb{R}^{1 \times 1 \times C_{out}}$.

$$z_{up_1} = UpResBlock(UpResBlock(UpResBlock(z_{1r}))) \quad (7)$$

$$z_{up_2} = UpResBlock(UpResBlock(z_{2r})) \quad (8)$$

$$z_{up_3} = UpResBlock(z_{3r}) \quad (9)$$

$$z_{up_4} = ResBlock(z_{4r}) \quad (10)$$

Equations (7), (8) and (9) illustrate the number of UpResBlocks required to match the output of the transformer layers to the CNN path layers, using three, two, and one UpResBlock for Tr_1 , Tr_2 and Tr_3 , respectively. For the Tr_4 layer, ResBlock is used instead of UpResBlock since no upsampling is required here, as depicted in equation (10).

On the other hand, the Encoders Fusion path has five layers which will be denoted by Un_1 , Un_2 , Un_3 , Un_4 and Un_5 , respectively. The first layer uses ResBlock on the input image $x \in \mathbb{R}^{H \times W \times C}$ to obtain the first encoder feature maps as shown in equation (11).

$$x_1 = ResBlock(x) \quad (11)$$

The second, third, fourth and fifth Encoders Fusion layers combine the transformer features with the max-pooled (MP) features of the previous CNN layer as shown in equations (12), (13), (14) and (15):

$$x_2 = ResBlock([z_{up_1}, MP(x_1)]) \quad (12)$$

$$x_3 = ResBlock([z_{up_2}, MP(x_2)]) \quad (13)$$

$$x_4 = ResBlock([z_{up_3}, MP(x_3)]) \quad (14)$$

$$x_5 = ResBlock([z_{up_4}, MP(x_4)]) \quad (15)$$

In our proposed D-TrAttUnet, dual decoders are used. As shown in Figure 2, the first decoder aims to segment the infection, while, the second one aims to segment the lungs regions. The objective of adding another decoder for lungs segmentation is to make the encoder concentrating inside the lungs, where the infection occurs. Furthermore, it allows to distinguish between lung and non-lung tissues, which can confuse the model, since the non-lung tissues may look similar to the infection, especially if the infection appears as a consolidation.

The bottleneck feature maps of the x_5 encoder are fed into the first expansion layer of the two decoders. First, x_5 is upsampled using a linear transformation to obtain d_5 , and then passed to the two decoders as shown in equation (16). On the other hand, the encoder feature maps x_1 , x_2 , x_3 and x_4 are fed to the two decoders layers of D-TrAttUnet through skip connections, as shown in Figure 2. Following the Att-Unet architecture [24], three linear upsampling layers (US), four decoder layers, four attention gates, and four ResBlocks are used for each decoder, as shown in the following equations:

$$d_5 = US(x_5) \quad (16)$$

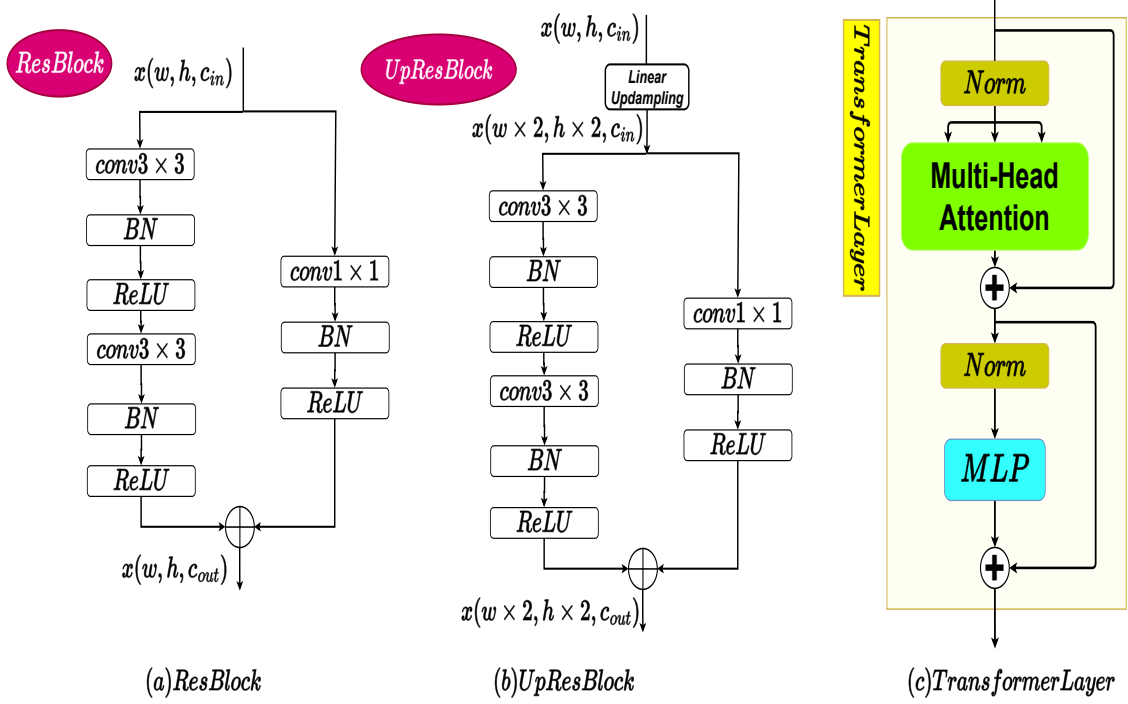


Figure 3: Description of ResBlock, UpResBlock and TransformerLayer.

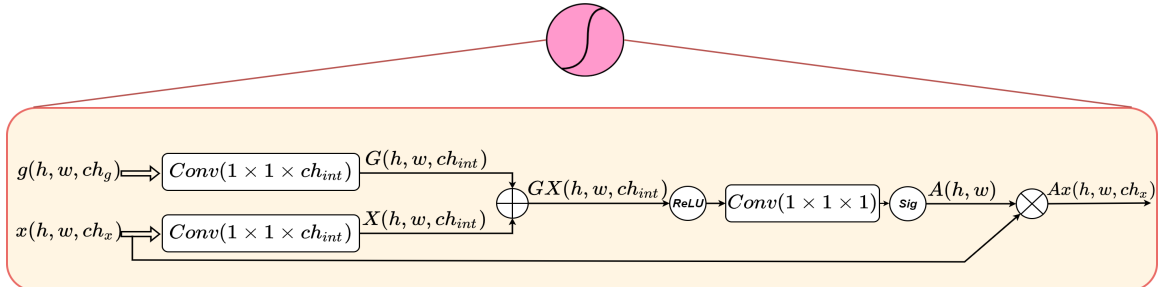


Figure 4: Attention Gate block, where g is the gating signal and the x is the input feature maps. $A(h, w)$ is the obtained spatial attention, which is applied for all channels of the input feature maps (x).

Table 1: The used datasets summary.

Name	Dataset	#CT-Scans	#Slices
Dataset_1	COVID-19 CT segmentation [48]	40	100
Dataset_2	Segmentation dataset nr. 2 [48]	9	829
Dataset_3	COVID-19-CT-Seg dataset [49]	20	3520

$$d_{41} = ResBlock([AttGate(x_4, US(x_5)); US(x_5)]) \quad (17)$$

$$d_{31} = ResBlock([AttGate(x_3, US(d_{41})); US(d_{41})]) \quad (18)$$

$$d_{21} = ResBlock([AttGate(x_2, US(d_{31})); US(d_{31})]) \quad (19)$$

$$d_{11} = ResBlock([AttGate(x_1, US(d_{21})); US(d_{21})]) \quad (20)$$

Similarly, d_{42} , d_{32} , d_{22} and d_{12} are obtained for the lung segmentation decoder. Finally, two convolutional 1 by 1 layers are used to match the feature map dimension of d_{11} and d_{12} to the infection and lungs masks prediction, which consist of a single channel for the lung and binary segmentation and three channels for the multi-classes segmentation.

The Attention Gate (AG) is depicted in Figure 4 [24], and it is defined as follows:

$$M_{att} = \psi_i(ReLU(BN(W_x x_i) + BN(W_g g_i))) \quad (21)$$

where $W_x \in \mathbb{R}^{1 \times 1 \times C_{int}}$ and $W_g \in \mathbb{R}^{1 \times 1 \times C_{int}}$ are two linear transformations that transform the channels c_x and c_g from x_i and g_i , respectively, to c_{int} . ψ_i consists of $W_{\psi_i} \in \mathbb{R}^{1 \times 1 \times 1}$ followed by BatchNormalization (BN) and sigmoid activation function to learn the spatial attention coefficient M_{att_p} for each pixel. The obtained spatial coefficients M_{att} are applied to the skip feature maps of the encoder x_i .

$$x_{att} = M_{att} x_i \quad (22)$$

4 Datasets and Evaluation Metrics

4.1 Datasets

Three publicly available datasets are used to evaluate the performance of our proposed approach for both binary and multi-classes segmentation tasks. Table 1 summarises the datasets used. Dataset_1 [48] consists of only 100 slices that show Covid-19 infection. These slices has lungs and multi-classes infection (GGO and Consolidation) masks.

Dataset_2 [48] consists of nine 3D CT-scans. In total, there are 829 slices, of which 373 slices show evidence of Covid-19 infection. This dataset was labelled by expert radiologists, where the masks of lungs, binary infection (non-infected and infected), and multi-classes labels (non-infected, GGO and Consolidation) were provided.

Dataset_3 [49] was constructed using 20 3D CT-scans. In total, Dataset_3 consists of 3520 slices, of which 1844 slices were labelled as infected by expert radiologists. Both lung regions and binary infection (non-infected and infected) masks were provided for each pixel by the radiologists.

For the binary segmentation task, both Dataset_2 and Dataset_3 are divided into 70%-30% splits, which are considered as training and testing splits, respectively. For the multi-classes segmentation task, Dataset_2 and 50% of Dataset_1 (50 slices) are used as the training data, the remaining 50 slices of Dataset_1 are used as the testing data.

Table 2: Performance evaluation of the proposed D-TrAttUnet and Unet [23], Att-Unet [24], Unet++ [25], CopleNet [12], AnamNet [13], and SCOATNet [10] on Dataset_2

Model	F1-S	D-S	IoU
Unet	47.36±14.54	22.23±6.51	32.24±12.76
Att-Unet	50.61±12.41	23.83±5.16	34.82±11.45
UNet++	55.20±12.14	27.01±5.75	39.05±10.96
CopleNet	60.92±9.16	26.09±4.11	44.42±9.44
AnamNet	38.87±3.8	20.13±1.66	27.20±2.91
SCOATNet	45.28±18.46	19.87±7.52	31.12±15.56
D-TrAttUnet	74.44±2.38	36.86±2.63	59.34±3.01

4.2 Evaluation Metrics

To evaluate the performance of different approaches, we used three evaluation metrics which are: F1-score (F1-S), Dice-score (D-S), Intersection over Union (IoU).

It should be noted that F1-score and Intersection over Union (IoU) are micro metrics, where they are calculated for all images at one time using True Positives (TP), True Negatives (TN), False Positives (FP) and False Negatives (FN). However, the Dice-score is the macro version of the $F1 - score$. For N training or test images, it is defined by:

$$\text{Dice-score} = 100 \cdot \frac{1}{N} \sum_{i=1}^N 2 \cdot \frac{TP_i}{2 \cdot TP_i + FP_i + FN_i} \quad (23)$$

where TP_i , TN_i , FP_i and FN_i are True Positives, True Negatives, False Positives and False Negative for the i th image, respectively.

5 Experiments and results

5.1 Experimental Setup

To produce our experiments, we mainly used Pytorch [50] library for deep learning. Each architecture is trained for 60 epochs with an initial learning rate of 0.1 which decays by 0.1 after 30 epochs, followed by another decay of 0.1 after 50 epochs. The batch size is set to 6 images and NVIDIA GPU Device GeForce TITAN RTX 24 GB is used. Three types of active data augmentation are used; random rotate with an angle between -35° and 35° with a probability of 10% and random Horizontal and vertical Flipping with probability of 20% for each. Adam is the used optimizer and Binary Cross Entropy and Cross Entropy are used as the losses for the Binary and Multi-classes segmentation tasks, respectively. It should be noted that the loss for the infection segmentation task is weighted by 0.7 and the loss for the lung segmentation is weighted by 0.3. The goal of giving more weight to the loss of the infection task is to have the training focus more on the infection segmentation task.

5.2 Binary Segmentation

In this section, we evaluate the performance of the proposed D-TrAttUnet and compare its performance with Unet [23], Att-Unet [24], Unet++ [25], CopleNet [12], AnamNet [13], and SCOATNet [10], it should be noted that each experiment was repeated five times. The results shown represent the average of the best result based on the F1-score on the validation data \pm the standard deviation of the five runs.

5.3 Multi-classes Segmentation

Table 4 summarizes the obtained results of our proposed D-TrAttUnet architecture and the comparison methods for multi-classes Covid-19 segmentation. For GGO, our approach outperforms the comparison architectures, where it is noticed that many of the comparison architectures achieved close results. Our architecture achieves better result than the best architecture for each metric; 1.44% for F_1 -score (Unet), 1.85% for Dice-score (AnamNet), and 1.58% for IoU (SCOATNET). Similarly, our approach surpasses the comparison methods for the consolidation segmentation. In more details, the proposed D-TrAttUnet architecture outperforms the best comparison architecture (which is SCOATNET) by 11.72%, 7.59% and 10.33% for F_1 -score, Dice-score, and IoU, respectively. These results show that our approach has a

Table 3: Performance evaluation of the proposed D-TrAttUnet and Unet [23], Att-Unet [24], Unet++ [25], CopleNet [12], AnamNet [13], and SCOATNet [10] on Dataset_3.

Model	F1-S	D-S	IoU
Unet	67.72±2.65	36.14± 1.31	51.25 ± 3
Att-Unet	62.85±7.06	33.51±2.5	46.19 ±7.03
UNet++	66.10 ±3.81	36.66±1.97	49.49±4.28
CopleNet	63.55±7.57	34.56±3.52	47.02±8.01
AnamNet	69.34±3.33	37.66±1.81	53.17±3.79
SCOATNet	70.27±2.39	38.47±0.56	54.22±2.86
D-TrAttUnet	75.42 ± 0.97	40.57 ± 0.28	60.55 ± 1.24

good capability to deal with unbalanced classes, which corresponds to the real scenario of Covid-19 infection, where GGO infection type is usually more frequent than consolidation.

Table 4: Performance evaluation of our proposed approach (D-TrAttUnet), Unet [23], Att-Unet [24], Unet++ [25], CopleNet [12], AnamNet [13], and SCOATNet [10] for multi-classes Covid-19 segmentation (No-infection, GGO and Consolidation).

Ex	Architecture	GGO			Consolidation		
		F1-S	D-S	IoU	F1-S	D-S	IoU
1	Unet	65.81±1.26	50.13±1.31	49.06±1.41	31.35±12.96	15.45±5.66	19.26±8.76
2	Att-Unet	64.81±1.89	50.44±1.35	47.97±2.06	39.04±6.81	19.26±3.55	24.48±5.31
2	Unet++	65.69±1.29	51.65±4.12	48.92±14.2	31.31±6.67	16.86±4.48	18.75±4.73
4	CopleNet	60.44±1.54	46.25±3.13	43.33±1.61	29.70±10.29	16.46±4.76	17.90±7.52
5	AnamNet	65.10± 3.56	51.69±4.81	48.36±3.82	31.97±6.12	18.06±4.61	19.18±4.36
6	SCOATNET	65.77±3.28	50.80±4.63	49.09±3.56	43.52±1.67	23.32±2.07	27.83±1.38
7	D-TrAttUnet	67.25±1.40	53.54± 1.24	50.67±1.59	55.24±0.97	30.91±1.67	38.16±0.93

5.4 Ablation Study

Table 5: Ablation study of Binary Segmentation scenario. The experimental results of Dataset_2 and Dataset_3 are summarized with investigating the effectiveness of the following components: Attention Gate (AG), Dual-Decoder (DD) and Transformer Encoder (TrEc).

Ex	Architecture	Ablation			Dataset_2		
		AG	DD	TrEc	F1-S	D-S	IoU
1	Unet (baseline)	✗	✗	✗	47.36±14.54	22.23± 6.51	32.24±12.76
2	AttUnet (baseline)	✓	✗	✗	50.61±12.41	23.83±5.16	34.82±11.45
3	D-TrUnet	✗	✓	✓	70.37± 3.98	36.46±2.56	54.43±4.80
4	D-AttUnet	✓	✓	✗	63.43± 6.35	30.39±4.08	46.76±6.81
5	TrAttUnet	✓	✗	✓	67.33±6.72	32.52±3.46	51.14±7.76
6	D-TrAttUnet	✓	✓	✓	74.44 ±2.38	36.86±2.63	59.34± 3.01

The aim of this section is to examine the significance of each element of the proposed D-TrAttUnet architecture. Tables 5 6 summarize the results on Dataset_2 and Dataset_3 for the binary segmentation, respectively. In this table, we study the importance of the Attention Gate (AG), the Dual Decoders (DD) and the Transformer Encoder (TrEc). From Experiments 1 and 2, it is noticed that the attention gate improves the results of Unet architecture in Dataset_2. In contrast, in Dataset_3, Unet’s results fell when the Attention Gate was added. This raises the question about the feasibility of using the attention gate for Covid-19 segmentation. To answer this question, we removed the attention gate from our approach in Experiment 3. By comparing the results of Experiment 3 and our proposed D-TrAttUnet architecture, we notice that the attention gate is very essential component in our approach, as the results on Dataset_2 improve by 4.07%, 0.4%, and 4.91% for F_1 -score, Dice-score, and IoU, respectively. Similarly, the results on Dataset_3 improve by 1%, 0.5%, and 1.28% for F_1 -score, Dice-score, and IoU, respectively. The integration of the transformer

Table 6: Ablation study of Binary Segmentation scenario. The experimental results of Dataset_2 and Dataset_3 are summarized with investigating the effectiveness of the following components: Attention Gate (AG), Dual-Decoder (DD) and Transformer Encoder (TrEc).

Ex	Architecture	Ablation			Dataset_3		
		AG	DD	TrEc	F1-S	D-S	IoU
1	Unet (baseline)	✗	✗	✗	67.72±2.65	36.14±1.31	51.25±3.01
2	AttUnet (baseline)	✓	✗	✗	62.85±7.06	33.51±2.5	46.19±7.03
3	D-TrUnet	✗	✓	✓	74.43±0.51	40.06±0.35	59.27±0.65
4	D-AttUnet	✓	✓	✗	72.21±0.53	38.88±0.79	56.51±0.64
5	TrAttUnet	✓	✗	✓	70.57±2.41	39.05±0.8	54.58±2.86
6	D-TrAttUnet	✓	✓	✓	75.42±0.97	40.57±0.28	60.55±1.24

layers in the encoding phase provides richer feature extraction, which is passed to the attention gate via the skip connections. The attention gates with richer features are properly activated to select the most important features from the encoder and the upsampled features of the previous decoder layer.

Experiment 4 (in Tables 5 6) depicts the results obtained when the transformer encoder is removed. From these results, it can be seen that without the transformer encoder, the results decreased, especially for the Dataset_2, which consists of only 9 CT-scans. In more details, the transformer encoder improves the results on Dataset_2 by 11%, 6.47%, and 12.58% for F_1 -score, Dice-score, and IoU, respectively. Similarly, the results of Dataset_3 are improved by 3.21%, 1.69%, and 4.04% for F_1 -score, Dice-score, and IoU, respectively. This proves the efficiency of combining the transformer and convolutional layers as encoder, especially when available data are limited, as is the case for pandemics.

The comparison between the results of experiment 5 and 6 (Tables 5 6) shows the importance of using Dual-Decoders. For both Dataset_2 and Dataset_3, the results are improved by adding the second decoder for lung segmentation at the same time as infection segmentation.

Table 7: Ablation study of Binary Segmentation scenario. The experimental results using Dataset_1 and Dataset_2 are summarized with investigating the effectiveness of the following components: Attention Gate (AG), Dual-Decoder (DD) and Transformer Encoder (TrEc).

Ex	Architecture	Ablation			GGO			Consolidation		
		AG	DD	TrEc	F1-S	D-S	IoU	F1-S	D-S	IoU
1	Unet (baseline)	✗	✗	✗	65.81±1.26	50.13±1.31	49.06±1.41	31.35±12.96	15.45±5.66	19.26±8.76
2	AttUnet (baseline)	✓	✗	✗	64.81±1.89	50.44±1.35	47.97±2.06	39.04±6.81	19.26±3.55	24.48±5.31
3	D-TrUnet	✗	✓	✓	63.77±1.69	49.80±2.97	46.83±1.82	50.39±2.08	29.19±4.55	33.71±1.84
4	D-AttUnet	✓	✓	✗	65.20±0.95	51.62±1.42	48.38±1.05	51.15±2.16	29.02±1.40	34.39±1.98
5	TrAttUnet	✓	✗	✓	65.69±1.29	51.65±4.12	48.92±1.42	48.15±1.75	27.23±4.52	31.73±1.50
6	D-TrAttUnet	✓	✓	✓	67.25±1.40	53.54±1.24	50.67±1.59	55.24±0.97	30.91±1.67	38.16±0.93

Table 7 depicts the ablation experiments for multi-classes segmentation. Similar to the ablation experiments of the binary segmentation, the importance of Attention Gate (AG), Dual Decoders (DD) and Transformer Encoder (TrEc) are studied in Table 7. From the results of Unet and AttUnet (Experiments 1 and 2), it can be observed that the attention gate is very useful for Consolidation segmentation, where the F_1 -score is improved by 8.7%. However, for GGO segmentation, adding the Attention Gate decreases the performance a little for F_1 -score and IoU. On the other hand, the Attention Gate turns out to be a very important component for both classes of segmentation (GGO and Consolidation) for our approach. More specifically, Attention Gate significantly improves the segmentation results of GGO by 3.48%, 3.74%, and 3.84% for F_1 -score, Dice-score, and IoU, respectively. Similarly, the results of consolidation are improved by 8.41%, 1.72%, and 4.45% for F_1 -score, Dice-score, and IoU, respectively. Similar to what found in the binary segmentation, the Attention Gate is also very important in multi-classes segmentation because it plays a crucial role in identifying the most important features from the encoder layers. Especially, that the multi-classes segmentation is a very complicated task compared to the binary segmentation task.

From the fourth and fifth rows of Table 7, it is very clear that both the Dual-Decoders and Transformer encoder are very important components for our proposed D-TrAttUnet architecture. The results are significantly improved by adding each of them. Where the results are considerable ameliorated by adding each element. The improvement is very significant in the consolidation segmentation, adding the Dual-Decoders and Transformer Encoder improves the F_1 -score results by about 4% and 6%, respectively. The ablation study in Tables 5 6, 7 proves the importance of each proposed component for binary and multi-classes Covid-19 segmentation for our approach.

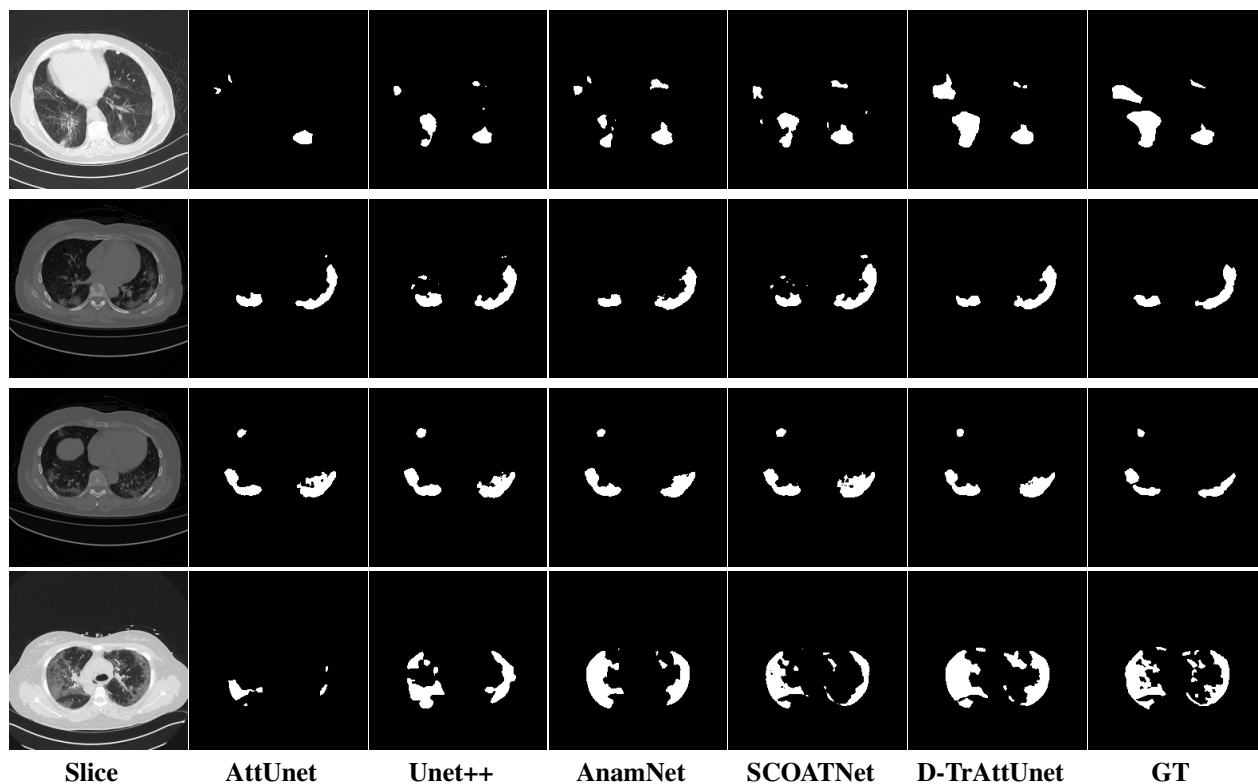


Figure 5: Visual comparison of a segmentation model trained with different segmentation architectures for Binary Covid-19 segmentation using Dataset_2 and Dataset_3.

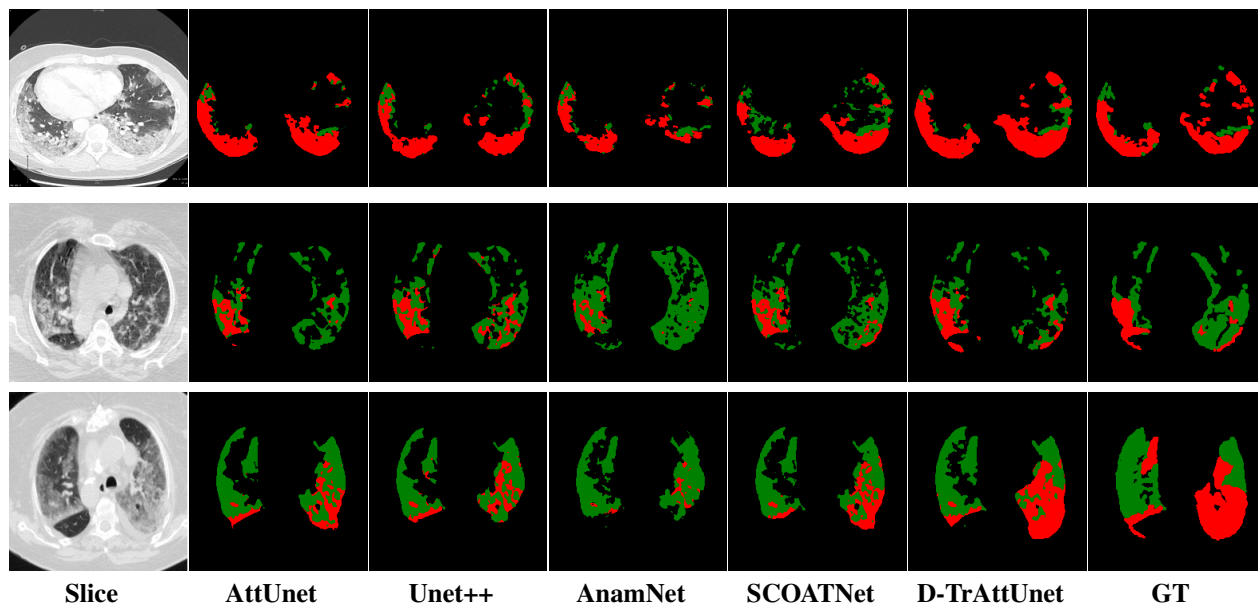


Figure 6: Visual comparison of a segmentation model trained with different segmentation architectures for Multi-classes (No-infection, GGO and Consolidation) Covid-19 infection segmentation using Dataset_1 and Dataset_2. GGO is presented by the Green color and Consolidation by the red color.

6 Discussion

In addition to comparing with state-of-the-art architectures, we visualize some predicted masks for both binary and multi-classes segmentation using our approach and the comparison methods, as shown in Figures 5 and 6. The comparison methods are: Att-Unet [24], Unet++ [25], AnamNet [13] and SCOATNet [10], which showed a competitive performance with our proposed approach (see Section 5).

The four visualized examples in Figure 5 are from the binary segmentation experiments of Dataset_2 and Dataset_3. The first example shows a case in which infection has spread to both lungs and appears as a GGO and small consolidation region at the bottom of the right lung. The comparison between the AttUnet mask and the ground truth (GT) shows that the AttUnet architecture fails in segmenting most of the infection regions. The Unet++, AnamNet and SCOATNet masks show improved segmentation performance compared to AttUnet. However, these architectures still miss some infected regions or segment lung tissues as infection instead. The mask of our proposed approach shows high similarity with GT in term of the number of regions and their global shape. Both examples 2 and 3 are cases where the infection has a peripheral distribution. The visualized masks show that the proposed D-TrAttUnet is the best architecture consistent with the ground truth. The fourth example depicts a severe case where the infection has spread to most of the lung regions.. The visualized masks exhibit that our proposed architecture performs better than the comparison architectures.

Figure 6 consists of the visualization of three examples masks using our approach and the comparison architectures for multi-classes Covid-19 segmentation. The first example shows a mixture case of GGO and Consolidation, where most of the infected regions consist of consolidation and small GGO regions are attached to the consolidation regions. Unlike the masks of the comparison architectures, the mask of our approach has a high similarity to the ground truth mask for both the consolidation and GGO classes. The second and third examples also represent a case where both GGO and consolidation are present in both lungs. The infected regions with consolidation are mainly in the lower lobes of both lungs and GGO spreads in both lungs with peripheral and posterior distribution. The masks of these examples confirm the observation in the first example, as the predicted masks of D-TrAttUnet show a high similarity to the GT masks for both infection types GGO and consolidation

7 Conclusion

In this paper, we proposed a CNN-Transformer based approach to segment Binary and Multi-classes Covid-19 infection from CT-scans. Our proposed D-TrAttUnet Encoder merges Transformer and CNN layers to extract richer local, global and long-range dependency features for Covid-19 segmentation. In addition, our proposed D-TrAttUnet architecture consists of Dual-Decoder, each one consists of attention gates, linear Upsampling and Convolutional blocks. The Dual-Decoders are used to segment the infection and the lung regions simultaneously.

To evaluate the performance of our approach, both Binary and multi-classes Covid-19 infection segmentation scenarios were investigated. The proposed D-TrAttUnet architecture outperformed three baseline architectures and three state-of-the-art architectures on three public Covid-19 segmentation datasets. The experimental results showed the importance of using attention gates with the compound CNN-Transformer encoder compared to a CNN-only Encoder. The ablation study showed the importance of each component of our proposed approach. Moreover, the combination of all proposed elements leads to better performance with stable and consistent results in both evaluated tasks (Binary and Multi-classes). As future work, we plan to evaluate the performance of our approach in similar segmentation tasks in medical imaging field.

References

- [1] Lauren M. Kucirka, Stephen A. Lauer, Oliver Laeyendecker, Denali Boon, and Justin Lessler. Variation in False-Negative rate of reverse transcriptase polymerase chain Reaction–Based SARS-CoV-2 Tests by time since exposure. *Annals of Internal Medicine*, 173(4):262–267, May 2020. Publisher: American College of Physicians.
- [2] Fares Bougourzi, Riccardo Contino, Cosimo Distanto, and Abdelmalik Taleb-Ahmed. Recognition of COVID-19 from CT Scans Using Two-Stage Deep-Learning-Based Approach: CNR-IEMN. *Sensors*, 21(17):5878, January 2021. Number: 17 Publisher: Multidisciplinary Digital Publishing Institute.
- [3] Ying-Hui Jin, Lin Cai, and Zhen-Shun et al. Cheng. A rapid advice guideline for the diagnosis and treatment of 2019 novel coronavirus (2019-nCoV) infected pneumonia (standard version). *Military Medical Research*, 7(1):4, February 2020.
- [4] Yu-Huan Wu, Shang-Hua Gao, and Jie et al. Mei. JCS: An Explainable COVID-19 Diagnosis System by Joint Classification and Segmentation. *IEEE Transactions on Image Processing*, 30:3113–3126, 2021. Conference Name: IEEE Transactions on Image Processing.

- [5] Fares Bougourzi, Cosimo Distanto, Fadi Dornaika, Abdelmalik Taleb-Ahmed, and Abdenour Hadid. ILC-Unet++ for Covid-19 Infection Segmentation. In Pier Luigi Mazzeo, Emanuele Frontoni, Stan Sclaroff, and Cosimo Distanto, editors, *Image Analysis and Processing. ICIAP 2022 Workshops*, Lecture Notes in Computer Science, pages 461–472, Cham, 2022. Springer International Publishing.
- [6] Edoardo Vantaggiato, Emanuela Paladini, Fares Bougourzi, Cosimo Distanto, Abdenour Hadid, and Abdelmalik Taleb-Ahmed. Covid-19 recognition using ensemble-cnns in two new chest x-ray databases. *Sensors*, 21(5), 2021.
- [7] Zhidan Li, Shixuan Zhao, Yang Chen, Fuya Luo, Zhiqing Kang, Shengping Cai, Wei Zhao, Jun Liu, Di Zhao, and Yongjie Li. A deep-learning-based framework for severity assessment of COVID-19 with CT images. *Expert Systems with Applications*, 185:115616, December 2021.
- [8] Fares Bougourzi, Cosimo Distanto, Abdelkrim Ouafi, Fadi Dornaika, Abdenour Hadid, and Abdelmalik Taleb-Ahmed. Per-COVID-19: A Benchmark Dataset for COVID-19 Percentage Estimation from CT-Scans. *Journal of Imaging*, 7(9):189, September 2021. Number: 9 Publisher: Multidisciplinary Digital Publishing Institute.
- [9] Deng-Ping Fan, Tao Zhou, and Ge-Peng et al. Ji. Inf-Net: Automatic COVID-19 Lung Infection Segmentation From CT Images. *IEEE Transactions on Medical Imaging*, 39(8):2626–2637, August 2020. Conference Name: IEEE Transactions on Medical Imaging.
- [10] Shixuan Zhao, Zhidan Li, and Yang et al. Chen. Scoat-net: A novel network for segmenting covid-19 lung opacification from ct images. *Pattern Recognition*, page 108109, 2021.
- [11] Fares Bougourzi, Cosimo Distanto, Fadi Dornaika, and Abdelmalik Taleb-Ahmed. Pdatt-unet: Pyramid dual-decoder attention unet for covid-19 infection segmentation from ct-scans. *Medical Image Analysis*, page 102797, 2023.
- [12] Guotai Wang, Xinglong Liu, Chaoping Li, and Zhiyong et al. Xu. A Noise-Robust Framework for Automatic Segmentation of COVID-19 Pneumonia Lesions From CT Images. *IEEE Transactions on Medical Imaging*, 39(8):2653–2663, August 2020. Conference Name: IEEE Transactions on Medical Imaging.
- [13] Naveen Paluru, Aveen Dayal, and Håvard Bjørke et al. Jenssen. Anam-Net: Anamorphic Depth Embedding-Based Lightweight CNN for Segmentation of Anomalies in COVID-19 Chest CT Images. *IEEE Transactions on Neural Networks and Learning Systems*, 32(3):932–946, March 2021. Conference Name: IEEE Transactions on Neural Networks and Learning Systems.
- [14] Ruxin Wang, Chaojie Ji, Yuxiao Zhang, and Ye Li. Focus, Fusion, and Rectify: Context-Aware Learning for COVID-19 Lung Infection Segmentation. *IEEE Transactions on Neural Networks and Learning Systems*, 33(1), January 2022. IEEE Transactions on Neural Networks and Learning Systems.
- [15] Omar Elharrouss, Nandhini Subramanian, and Somaya Al-Maadeed. An Encoder–Decoder-Based Method for Segmentation of COVID-19 Lung Infection in CT Images. *SN Computer Science*, 3(1):13, October 2021.
- [16] F. Bougourzi, F. Dornaika, and A. Taleb-Ahmed. Deep learning based face beauty prediction via dynamic robust losses and ensemble regression. *Knowledge-Based Systems*, 242:108246, April 2022.
- [17] Fares Bougourzi, Fadi Dornaika, Nagore Barrena, Cosimo Distanto, and Abdelmalik Taleb-Ahmed. CNN based facial aesthetics analysis through dynamic robust losses and ensemble regression. *Applied Intelligence*, August 2022.
- [18] Vivek Kumar Singh, Mohamed Abdel-Nasser, Nidhi Pandey, and Domenech Puig. LungINFseg: Segmenting COVID-19 Infected Regions in Lung CT Images Based on a Receptive-Field-Aware Deep Learning Framework. *Diagnostics*, 11(2):158, February 2021. Number: 2 Publisher: Multidisciplinary Digital Publishing Institute.
- [19] Issam Laradji, Pau Rodriguez, and Oscar et al. Manas. A weakly supervised consistency-based learning method for covid-19 segmentation in ct images. In *Proceedings of the IEEE/CVF Winter Conference on Applications of Computer Vision (WACV)*, pages 2453–2462, January 2021.
- [20] Zhonghua Sun, Nan Zhang, Yu Li, and Xunhua Xu. A systematic review of chest imaging findings in COVID-19. *Quantitative Imaging in Medicine and Surgery*, 10(5):1058–1079, May 2020.
- [21] Sana Salehi, Aidin Abedi, Sudheer Balakrishnan, and Ali Gholamrezanezhad. Coronavirus disease 2019 (COVID-19): a systematic review of imaging findings in 919 patients. *Ajr Am J Roentgenol*, 215(1):87–93, 2020.
- [22] Jiannan Liu, Bo Dong, Shuai Wang, Hui Cui, Deng-Ping Fan, Jiquan Ma, and Geng Chen. COVID-19 lung infection segmentation with a novel two-stage cross-domain transfer learning framework. *Medical Image Analysis*, 74:102205, 2021.
- [23] Olaf Ronneberger, Philipp Fischer, and Thomas Brox. U-Net: Convolutional Networks for Biomedical Image Segmentation. In *Medical Image Computing and Computer-Assisted Intervention – MICCAI 2015*, Lecture Notes in Computer Science, pages 234–241, Cham, 2015. Springer International Publishing.

- [24] Ozan Oktay, Jo Schlemper, and Loic Le et al. Folgoc. Attention U-Net: Learning Where to Look for the Pancreas. *arXiv:1804.03999 [cs]*, May 2018. arXiv: 1804.03999.
- [25] Zongwei Zhou, Md Mahfuzur Rahman Siddiquee, Nima Tajbakhsh, and Jianming Liang. UNet++: A Nested U-Net Architecture for Medical Image Segmentation. In Danail Stoyanov, Zeike Taylor, and Gustavo et al. Carneiro, editors, *Deep Learning in Medical Image Analysis and Multimodal Learning for Clinical Decision Support*, Lecture Notes in Computer Science, pages 3–11, Cham, 2018. Springer International Publishing.
- [26] Alex Krizhevsky, Ilya Sutskever, and Geoffrey E Hinton. ImageNet Classification with Deep Convolutional Neural Networks. In *Advances in Neural Information Processing Systems*, volume 25. Curran Associates, Inc., 2012.
- [27] Jia Deng, Wei Dong, Richard Socher, Li-Jia Li, Kai Li, and Li Fei-Fei. ImageNet: A large-scale hierarchical image database. In *2009 IEEE Conference on Computer Vision and Pattern Recognition*, pages 248–255, June 2009. ISSN: 1063-6919.
- [28] Yao Zhou, Gary G. Yen, and Zhang Yi. Evolutionary Compression of Deep Neural Networks for Biomedical Image Segmentation. *IEEE Transactions on Neural Networks and Learning Systems*, 31(8):2916–2929, August 2020. Conference Name: IEEE Transactions on Neural Networks and Learning Systems.
- [29] Nikhil Kumar Tomar, Debesh Jha, Michael A. Riegler, Håvard D. Johansen, Dag Johansen, Jens Rittscher, Pål Halvorsen, and Sharib Ali. FANet: A Feedback Attention Network for Improved Biomedical Image Segmentation. *IEEE Transactions on Neural Networks and Learning Systems*, pages 1–14, 2022. Conference Name: IEEE Transactions on Neural Networks and Learning Systems.
- [30] Zhengxin Zhang, Qingjie Liu, and Yunhong Wang. Road Extraction by Deep Residual U-Net. *IEEE Geoscience and Remote Sensing Letters*, 15(5):749–753, May 2018. Conference Name: IEEE Geoscience and Remote Sensing Letters.
- [31] Salman Khan, Muzammal Naseer, Munawar Hayat, Syed Waqas Zamir, Fahad Shahbaz Khan, and Mubarak Shah. Transformers in vision: A survey. *ACM Computing Surveys (CSUR)*, 2021. Publisher: ACM New York, NY.
- [32] Alexey Dosovitskiy, Lucas Beyer, Alexander Kolesnikov, Dirk Weissenborn, Xiaohua Zhai, Thomas Unterthiner, Mostafa Dehghani, Matthias Minderer, Georg Heigold, and Sylvain Gelly. An image is worth 16x16 words: Transformers for image recognition at scale. *arXiv preprint arXiv:2010.11929*, 2020.
- [33] Ze Liu, Yutong Lin, Yue Cao, Han Hu, Yixuan Wei, Zheng Zhang, Stephen Lin, and Baining Guo. Swin transformer: Hierarchical vision transformer using shifted windows. In *Proceedings of the IEEE/CVF International Conference on Computer Vision*, pages 10012–10022, 2021.
- [34] Hugo Touvron, Matthieu Cord, Matthijs Douze, Francisco Massa, Alexandre Sablayrolles, and Herve Jegou. Training data-efficient image transformers and distillation through attention. In Marina Meila and Tong Zhang, editors, *Proceedings of the 38th International Conference on Machine Learning*, volume 139 of *Proceedings of Machine Learning Research*, pages 10347–10357. PMLR, 18–24 Jul 2021.
- [35] Fahad Shamsad, Salman Khan, Syed Waqas Zamir, Muhammad Haris Khan, Munawar Hayat, Fahad Shahbaz Khan, and Huazhu Fu. Transformers in Medical Imaging: A Survey, January 2022. arXiv:2201.09873 [cs, eess].
- [36] Yin Dai, Yifan Gao, and Fayu Liu. TransMed: Transformers Advance Multi-Modal Medical Image Classification. *Diagnostics*, 11(8):1384, August 2021. Number: 8 Publisher: Multidisciplinary Digital Publishing Institute.
- [37] Zhiqiang Shen, Rongda Fu, Chaonan Lin, and Shaohua Zheng. COTR: Convolution in Transformer Network for End to End Polyp Detection. In *2021 7th International Conference on Computer and Communications (ICCC)*, pages 1757–1761, December 2021.
- [38] Ali Hatamizadeh, Yucheng Tang, Vishwesh Nath, Dong Yang, Andriy Myronenko, Bennett Landman, Holger R. Roth, and Daguang Xu. UNETR: Transformers for 3D Medical Image Segmentation. pages 574–584, 2022.
- [39] Huisi Wu, Shihuai Chen, Guilian Chen, Wei Wang, Baiying Lei, and Zhenkun Wen. FAT-Net: Feature adaptive transformers for automated skin lesion segmentation. *Medical Image Analysis*, 76:102327, February 2022.
- [40] Olivier Petit, Nicolas Thome, Clement Rambour, Loic Themyr, Toby Collins, and Luc Soler. U-Net Transformer: Self and Cross Attention for Medical Image Segmentation. In Chunfeng Lian, Xiaohuan Cao, Islem Rekik, Xuanang Xu, and Pingkun Yan, editors, *Machine Learning in Medical Imaging*, Lecture Notes in Computer Science, pages 267–276, Cham, 2021. Springer International Publishing.
- [41] Wenxuan Wang, Chen Chen, Meng Ding, Hong Yu, Sen Zha, and Jianguyun Li. TransBTS: Multimodal Brain Tumor Segmentation Using Transformer. In Marleen de Bruijne, Philippe C. Cattin, Stéphane Cotin, Nicolas Padoy, Stefanie Speidel, Yefeng Zheng, and Caroline Essert, editors, *Medical Image Computing and Computer Assisted Intervention – MICCAI 2021*, Lecture Notes in Computer Science, pages 109–119, Cham, 2021. Springer International Publishing.

- [42] Jie Hu, Li Shen, and Gang Sun. Squeeze-and-Excitation Networks. pages 7132–7141, 2018.
- [43] Stephanie A. Harmon, Thomas H. Sanford, Sheng Xu, Evrim B. Turkbey, Holger Roth, Ziyue Xu, Dong Yang, Andriy Myronenko, Victoria Anderson, Amel Amalou, Maxime Blain, Michael Kassin, Dilara Long, Nicole Varble, Stephanie M. Walker, Ulas Bagci, Anna Maria Ierardi, Elvira Stellato, Guido Giovanni Plensich, Giuseppe Franceschelli, Cristiano Girlando, Giovanni Irmici, Dominic Labella, Dima Hammoud, Ashkan Malayeri, Elizabeth Jones, Ronald M. Summers, Peter L. Choyke, Daguang Xu, Mona Flores, Kaku Tamura, Hirofumi Obinata, Hitoshi Mori, Francesca Patella, Maurizio Cariati, Gianpaolo Carrafiello, Peng An, Bradford J. Wood, and Baris Turkbey. Artificial intelligence for the detection of COVID-19 pneumonia on chest CT using multinational datasets. *Nature Communications*, 11(1):4080, August 2020. Number: 1 Publisher: Nature Publishing Group.
- [44] Afshar Shamsi, Hamzeh Asgharnezhad, Shirin Shamsi Jokandan, Abbas Khosravi, Parham M. Kebria, Darius Nahavandi, Saeid Nahavandi, and Dipti Srinivasan. An Uncertainty-Aware Transfer Learning-Based Framework for COVID-19 Diagnosis. *IEEE Transactions on Neural Networks and Learning Systems*, 32(4):1408–1417, April 2021. Conference Name: IEEE Transactions on Neural Networks and Learning Systems.
- [45] Ying Chen, Taohui Zhou, Yi Chen, Longfeng Feng, Cheng Zheng, Lan Liu, Liping Hu, and Bujian Pan. HADCNet: Automatic segmentation of COVID-19 infection based on a hybrid attention dense connected network with dilated convolution. *Computers in Biology and Medicine*, 149:105981, October 2022.
- [46] Jiannan Liu, Bo Dong, Shuai Wang, Hui Cui, Deng-Ping Fan, Jiquan Ma, and Geng Chen. Covid-19 lung infection segmentation with a novel two-stage cross-domain transfer learning framework. *Medical Image Analysis*, 74:102205, 2021.
- [47] Ashish Vaswani, Noam Shazeer, Niki Parmar, Jakob Uszkoreit, Llion Jones, Aidan N. Gomez, \Lukasz Kaiser, and Illia Polosukhin. Attention is all you need. *Advances in neural information processing systems*, 30, 2017.
- [48] RADIOLOGISTS. COVID-19 CT-scans segmentation datasets, available at: "<http://medicalsegmentation.com/covid19>", 2019. Last visited: 18-08-2021.
- [49] Jun Ma, Yixin Wang, Xingle An, and et al. Toward data efficient learning: A benchmark for COVID 19 CT lung and infection segmentation. *Medical Physics*, 48:1197–1210, March 2021.
- [50] Adam Paszke, Sam Gross, and Francisco et al. Massa. Pytorch: An imperative style, high-performance deep learning library. In *Advances in neural information processing systems*, pages 8026–8037, 2019.